* Prepared for AIChE ~~national~~ NATL. meeting,
San Juan, Puerto Rico,
Sept. 29 - Oct. 2, 1963
~~and AIChE Journal~~

Submitted for Publication [redacted]

39 p.

MONTE CARLO SOLUTION OF RADIANT HEAT TRANSFER IN A NONGREY NONISOTHERMAL GAS WITH TEMPERATURE-DEPENDENT PROPERTIES

By John R. Howell and Morris Perlmutter [1963]

Lewis Research Center
National Aeronautics and Space Administration
Cleveland, Ohio

ABSTRACT

15234

The Monte Carlo method is applied to the problem of determining the radiant heat transfer and emissive power distribution in an absorbing emitting nongrey gas with temperature-dependent properties contained between infinite parallel black walls. The gas emissive power distribution is presented for the cases of no heat source and a parabolic distribution of heat sources in the gas. Calculations are carried out for hydrogen at temperatures in the range 5000° to 12,000° K. A comparison is made with various approximate methods and to the limiting diffusion and transparent solutions. The results indicate that the approximate solutions may be in considerable error.

INTRODUCTION

The problem of radiative heat transfer in a gas-filled enclosure is of considerable interest. The grey-gas assumption generally used can be in error for several reasons: The total absorptivity of a real gas generally does not follow the exponential absorption law. There is difficulty in choosing the appropriate mean absorption coefficient for a specific case. If there are large temperature variations in the gas or between the gas and a wall, significant errors can occur because of the changing distribution of energy with wavelength. A grey-gas assumption, with total absorptivity taken equal to total emissivity in the gas, cannot account for these effects. Ignoring the variation of absorption coefficient with temperature can also lead to considerable error.

The problem of radiative transfer to real gases has been treated previously by Hottel and Cohen [1], who have presented a method based on separating a gas volume into finite isothermal elements and solving the resulting set of transfer equations. The real gas properties are approximated by fitting a summation of exponential terms.

Another treatment of the problem is given by Bevans and Dunkle [2]. The band approximation is used for the properties, and finite isothermal elements are assumed. The solution is obtained by the network method.

Deissler [3] extended the diffusion approximation with jump boundary conditions to the case of real gases but, as in [1] and [2], does not fully account for the effect of temperature on the gas properties.

Some recent papers [4], [5] have applied the Monte Carlo method used previously in the fields of rarefied gas dynamics and nuclear transport to heat radiation problems involving grey gases. Monte Carlo is applied herein to a nonisothermal gas radiative transfer problem where the absorption coefficient is allowed to vary with both wavelength and temperature. A comparison is made with the modified diffusion approximation including temperature effects on the absorption coefficient; with the temperature dependent grey-gas solution; with the temperature independent nongrey gas solution; and with the transparent approximation.

The procedure consists of following a "bundle"* of energy through a probable path until final absorption in the system. Enough such bundles are followed to give statistically meaningful results.

NOMENCLATURE

C_1 constant in Planck energy distribution, 5.9529×10^{-16} (kw)(cm^2)

C_2 constant in Planck energy distribution, 1.4387 (cm)($^{\circ}$K)

c energy per bundle, kw

D distance between infinite parallel plates, cm

e emissive power, kw/cm^2

$e_{b\lambda}$ Planck black-body emission distribution; $\dfrac{2\pi C_1}{\lambda^5\left[\exp\left(\dfrac{C_2}{\lambda T}\right) - 1\right]}$

G heat generation rate per unit volume, kw/cm^3

i increment index

l bundle path length to point of absorption nondimensionalized by D

N total number of bundles originally emitted per unit area

q energy per unit area, kw/cm^2

R randomly chosen number in range from 0 to 1

S number of bundles per unit area

T temperature, $^{\circ}$K

x normal distance from surface 0, nondimensionalized by D

*These bundles cannot be considered photons since the energy per bundle does not depend on wavelength. They rather represent a group or bundle of photons at a given wavelength such that all bundles have equal energy.

ϵ emissivity

η angle to normal of surfaces

κ gas absorption coefficient, cm^{-1}

λ wavelength, cm

σ Stefan-Boltzmann constant, 5.670×10^{-15} $kw/(cm^2)(^oK^4)$

τ optical thickness; κD

τ_P Planck mean optical thickness (eq. (10))

τ_R Rosseland mean optical thickness (eq. (B13))

Subscripts:

A surface

A-Δx originally emitted at A, absorbed in Δx

b black: wall emissivity of 1

g gas

i gas increment number

max maximum value

t total

w of the wall

x at point x

Δx gas increment

λ wavelength dependent

0 of surface 0

0-1 emitted at 0, absorbed at 1

1 of surface 1

Superscript:

— bar over any term denotes value integrated over wavelength range $\Delta\lambda$

ANALYSIS

The radiant energy transfer and the temperature distribution are found for a nongrey nonisothermal gas between infinite parallel walls. Only the case of black walls will be treated, but extension to nongrey walls is straightforward. The refractive index of the gas is assumed to be 1. Two solutions are obtained: one for the walls at unequal temperatures and with no heat sources in the gas and the other for both walls at the same temperature and a parabolic distribution of heat sources in the gas. The geometry studied is shown in figure 1.

No energy source in the gas. - The computer flow chart for this case is shown in figure 2.

As derived in appendix A (eq. (A4)), when a bundle is emitted from wall 0 ⟨1⟩*, its wavelength is determined from

$$R = \frac{\int_0^{\lambda} \epsilon_{\lambda 0} e_{b\lambda 0} \, d\lambda}{\int_0^{\infty} \epsilon_{\lambda 0} e_{b\lambda 0} \, d\lambda} \tag{1}$$

where R is a random number in the range 0 to 1, $\epsilon_{\lambda 0}$ is the emissivity, and $e_{b\lambda 0}$ the black emissive power distribution of surface 0. By integration of (1), a relation $\lambda = F_0(R)$ is obtained for a given surface temperature.

If the surface is assumed to emit diffusely, the direction of the emitted bundle is shown in reference [4] to be

*The numbers in brackets ⟨⟩ correspond to those in figure 2.

$$\cos\,\eta = \sqrt{R_1} \qquad (2)$$

The distance the bundle travels before absorption in the gas is given in appendix A by equation (A9) as

$$\ln R = -\int_0^l \tau_\lambda\, dl' \qquad (3)$$

where $\tau_\lambda = D\kappa_\lambda$ is the monochromatic gas optical thickness. If it is assumed that the gas is divided into $1/\Delta x$ increments, each with an absorption coefficient $\kappa_{\lambda,i}$, the increment i in which absorption occurs can be found by writing (3) as

$$\ln R + \frac{\Delta x}{\sqrt{R_1}} \sum_{z=1}^{i} \tau_{\lambda,z} > 0 \qquad (4)$$

and carrying out the summation until the inequality is satisfied $\langle 2 \rangle$. Since the absorption coefficient is temperature dependent, solution of (4) requires a priori knowledge of the temperature distribution across the channel. This necessitates an iterative procedure.

If the increment number i is greater than the number of increments available $\langle 3 \rangle$, then the bundle must be absorbed by black surface 1. If the bundle is absorbed in the gas, then the normal distance from surface 0 at which absorption occurs, x, is found $\langle 5 \rangle$. The bundle is tallied as being absorbed in increment i $\langle 6 \rangle$. Since the gas is at the steady state, a new bundle must be emitted from x. Its wavelength is determined from $\lambda = F_{g,x}(R)$, $\langle 7 \rangle$, as calculated from equation (A5) in appendix A. The direction of emission from any point x in the gas is shown in reference [4] to be given by

$$\cos\,\eta = 1 - 2R_2 \qquad (5)$$

This direction is examined to determine whether it is toward surface 0 or surface 1 ⟨8⟩. A check is made to determine whether the bundle is reabsorbed in the same increment i ⟨9⟩. If so, the new point of absorption x is found ⟨10⟩, ⟨11⟩ and the bundle is again tallied and reemitted ⟨6⟩, etc. If not, the increment I in which it is absorbed is calculated ⟨12⟩, again by modifying equation (3). A check is made of the increment number ⟨13⟩ to see whether the bundle reached the wall. If so, it is tallied at that wall, ⟨14⟩. If not, the point of absorption x is calculated ⟨11⟩, and the bundle is tallied ⟨6⟩ and reemitted as before. The procedure is followed until absorption at a wall. Enough such paths are traced to give statistically meaningful results.

A similar procedure is then followed for those bundles emitted from surface 1.

The net energy transferred to surface 1 is

$$(q_{0-1})_{net} = c_0 S_{0-1} - c_1 S_{1-0} \tag{6}$$

where S_{A-B} is defined as the number of bundles emitted at surface A per unit area that are absorbed at surface B. The term c_A is the energy per bundle emitted from surface A, and is defined by

$$c_A N_A = \int_0^\infty \epsilon_{\lambda A} e_{b\lambda,A}\, d\lambda \tag{7}$$

where N_A is the total number of bundles emitted per unit area from A. For the case of black walls, equation (6) becomes

$$\left[\frac{(q_{0-1})_{net}}{e_{b0} - e_{b1}}\right]_{G(x)=0} = \frac{1}{1 - \left(\frac{e_{b1}}{e_{b0}}\right)} \left[\frac{S_{0-1}}{N_0} - \left(\frac{e_{b1}}{e_{b0}}\right)\frac{S_{1-0}}{N_1}\right] \tag{8}$$

The emissive power of a gas volume of width Δx is obtained from the number of bundles emitted in the gas volume:

$$4\,\Delta x \int_0^\infty e_{g,\lambda,i}\tau_{\lambda,i}\,d\lambda = \left(\frac{S_{0-\Delta x,i}}{N_0}\right) e_{b0} + \left(\frac{S_{1-\Delta x,i}}{N_1}\right) e_{b1} = 4\,\Delta x\,\tau_{P,i}e_{g,i} \tag{9}$$

where $S_{A-\Delta x,i}$ is the number of bundles absorbed and therefore reemitted in the volume element i of width Δx that originated at surface A, and $\tau_{P,i}$ is the Planck mean optical thickness in increment i and is defined as

$$\tau_P = \frac{\int_0^\infty \tau_\lambda e_{g,\lambda}\,d\lambda}{e_g} \tag{10}$$

The emissive power distribution in the gas is then

$$\left(\frac{e_{g,i} - e_{b0}}{e_{b1} - e_{b0}}\right)_{G(x)=0} = \frac{1}{\left(1 - \frac{e_{b1}}{e_{b0}}\right)}\left\{1 - \frac{1}{4\tau_{P,i}\,\Delta x}\left[\frac{S_{0-\Delta x,i}}{N_0} + \left(\frac{S_{1-\Delta x,i}}{N_1}\right)\frac{e_{b1}}{e_{b0}}\right]\right\} \tag{11}$$

Gas with parabolic source distribution between plates at equal temperatures. - The flow chart for this case is also shown in figure 2. A parabolic distribution of heat sources of the form

$$G(x) = 4G_{max}x(1 - x) \tag{12}$$

is assumed, where G is the heat generation rate per unit volume. The problem is to find the emissive power distribution in the gas.

The emissive power is related to the number of emissions in the gas by

$$4\tau_{P,i}\ \Delta x\ e_{g,i} = c_g(S_{g,\Delta x})_i + c_0(S_{0-\Delta x})_i + c_1(S_{1-\Delta x})_i \tag{13}$$

where $(S_{g,\Delta x})_i$ is the total number of bundles emitted in a volume element Δx around point i and includes original emissions and reemissions after absorption of bundles originating in other elements. The last two terms give the energy absorbed from the walls.

The energy per bundle originally emitted in the gas c_g is defined as

$$c_g = \frac{D\int_0^1 G(x')dx'}{N_g} = \frac{2G_{max}D}{3N_g} \tag{14}$$

where N_g is the total number of bundles originally emitted in the gas.

From the assumption of equal wall temperatures we can reduce equation (11) to the identity

$$4\tau_{P,i}\ \Delta x = \frac{S_{0-\Delta x,i}}{N_0} + \frac{S_{1-\Delta x,i}}{N_1}$$

Substituting this relation into equation (13) gives

$$\left[\frac{e_{g,i} - e_b}{\left(\frac{2G_{max}D}{3}\right)}\right]_{T_0=T_1} = \frac{(S_{g,\Delta x})_i}{4N_g\ \Delta x\ \tau_{P,i}} \tag{15}$$

The Monte Carlo program is essentially that described in the previous section except that bundles originate within the gas at points determined by the function $x = F_S(R)$, as derived in appendix A (eq. (A11)), rather than at the surfaces.

Sample problem. - The calculations were carried out for hydrogen in the temperature range of 5000° to 12,000° K. The absorption coefficient as a function of temperature and wavelength used in the problem is shown in figure 3(a). The mean absorption coefficients calculated from this data and used in the comparison solutions are shown in figure 3(b). The data is from reference [6], and is based on analytical calculations. The absorption coefficient was assumed zero outside the range $\lambda_{min} < \lambda < \lambda_{max}$.

The Monte Carlo solution is compared with the diffusion solution with jump boundary conditions for this specific problem. The diffusion solution given in appendix B follows Deissler [3] but extends his results to include the variation of absorption coefficient across the channel.

The diffusion solution uses the Rosseland mean absorption coefficient κ_R as defined by equation (B13). If the absorption coefficient is very small over parts of the spectrum, the value of κ_R is weighted excessively by this portion of the spectrum. Because of this, the problem must be solved in two parts. Over the spectrum range with appreciable absorption coefficient the diffusion solution is used, and over the remainder the gas is considered transparent.

The results for the example are also compared with the Monte Carlo temperature-dependent solution based on the Planck mean absorption coefficient of the gas in each increment as defined by equation (10), and with the Monte Carlo solution using the wavelength-dependent absorption coefficient evaluated at an average temperature. Limiting exact solutions for optically thick and transparent gases are also given.

RESULTS

No gas heat sources. - The net heat transferred between the heated infinite black plates enclosing hydrogen is shown in figure 4. The temperature of plate 0 was taken as 9500° K, and of plate 1 as 4500° K. The results are shown for different values of plate spacing D. The gas was assumed transparent at wavelengths less than 0.15×10^{-4} or greater than 2×10^{-4} cm.

Comparison of the exact Monte Carlo solution to the wavelength-dependent, temperature-independent absorption coefficient $\kappa(\lambda, T_c)$ solution shows a lower heat-transfer rate for the exact solution. This is because the wavelength-dependent gas absorption coefficient is evaluated at 7000° K, the average of the wall temperatures. However, the larger slope of the curve of gas absorption coefficient with temperature (fig. 3(b)) near the higher wall temperature indicates that a higher mean gas temperature should be used to evaluate $\kappa(\lambda, T_c)$ for this case.

Also shown is the Monte Carlo solution using a temperature-dependent Planck mean absorption coefficient, $\kappa_P(T)$, which gives lower heat transfer than the exact solution because the mean absorption coefficients are weighted according to the Planck energy distribution based on the local gas temperature (eq. (10)). This gives most weight to the absorption coefficient in the wavelengths where the local Planck energy distribution is a maximum. The energy absorbed locally, however, will have a wavelength distribution based on its source energy spectrum. In the present case, this gives an exaggerated absorption coefficient for calculating the energy absorbed from the hot wall and a consequently smaller heat transfer than the exact solution.

The modified diffusion solution derived in appendix B is in close agreement with the Monte Carlo solution using the Planck mean absorption coefficient. This agreement might be expected, since both solutions are based on a temperature-dependent mean absorption coefficient. The diffusion solution is in better agreement with the exact solution as the plate spacing is increased. The approximation of the temperature dependence of the absorption coefficient as a parabolic form, however, still introduces some error.

The gas emissive power distributions for various plate spacings are shown in figure 5. The local gas emissive power is dependent on the temperature surroundings viewed and the absorption coefficient. For the example shown, elements near the hot wall attain equilibrium temperatures close to the hot wall temperature. Elements near the cold wall are less readily influenced by the hot wall, especially for large plate spacing, because the large absorption coefficient in the hotter portion of the gas masks the hot wall. This leads to the large emissive power gradient near the hot wall for cases with temperature-dependent absorption coefficient.

In figure 5(a), the exact solutions for various plate spacings are shown. The limiting solutions $D \to \infty$ and $D \to 0$ are given in appendixes B and C, respectively. As the plate spacings get larger, the jump between the emissive powers of the wall and the gas at the wall become smaller and approach zero as the plate spacing becomes very large. As the plate spacing approaches zero, the emissive power becomes constant since any gas element views both walls equally well. The constant is not the average of the emissive powers of the walls as would be the case for a grey gas. The reason is that the wavelength-dependent absorption coefficient is lower for the wavelengths of energy leaving the hot wall and is comparatively large at the wavelengths of local gas emission, which leads in turn to an equilibrium temperature nearer that of the cold wall.

Figures 5(b) and (c) compare the exact Monte Carlo solutions with various approximate solutions at two plate spacings. The agreement is seen to be better at a small plate spacing, since the temperature range, and therefore the variation in absorption coefficient with temperature, is less. The wavelength-dependent, temperature-independent absorption coefficient solution gives emissive power distributions with less slope at the hot wall than the exact solution, since there is no temperature effect on the absorption coefficient.

The temperature-dependent Monte Carlo solution using a Planck mean absorption coefficient gives curves of shape similar to the exact solution, but of higher values of gas temperature. This is again due to the erroneously high absorption of energy in each element because of the large mean absorption coefficient computed on the basis of the local gas temperature. This effect becomes smaller for optically thick gases.

The slope near the walls for the modified diffusion solution does not correspond to the exact solution, especially at the smaller plate spacing, because the effects of the wall are only included in the emissive power jump at the wall, and not in the gas away from the wall. As the plate spacing becomes larger, this approximation improves. At the cold wall, however, the results are still poor because of the low absorption coefficient there.

Parabolic heat source in the gas. - For a symmetrical distribution of heat sources between black walls at equal temperatures, the heat transferred to each wall is equal to one-half the total heat generated.

The emissive power distribution in the gas is shown in figure 6(a) for the exact solutions for various values of the plate spacing D. The limiting transparent solution is given in appendix C. The gas temperatures become higher at larger plate spacing because of the increasing difficulty of transferring heat to the walls from positions near the centerline.

In figures 6(b) and (c), the simplified solutions are compared with the exact solution for a large and small plate spacing.

The various approximate Monte Carlo solutions give excellent agreement to the exact solution for the smaller plate spacing because of the small temperature variations in the enclosure.

The diffusion solution gives better agreement with increasing plate spacing and higher temperatures, where the absorption coefficients are larger. In figure 7, the difference between the gas centerline and wall emissive powers is plotted for the exact Monte Carlo solution. This is compared to the two limiting solutions: The diffusion solution, applicable for large plate spacing, and the transparent approximation for small plate spacing. The exact solution is seen to approach the limiting solutions.

CONCLUSIONS

The results indicate that for gases with large optical thickness the diffusion approximation modified for temperature-dependent absorption coefficient is applicable. In the other extreme, the transparent solutions are applicable. It may be possible in certain cases to divide the energy spectrum so that different solutions are used in different regions.

In general, however, the diffusion or transparent assumptions or the use of temperature and/or wavelength independent absorption coefficients can lead to very misleading results. In addition, it is very difficult to predict the magnitude or sign of the error, since it will strongly depend on the properties of the particular gas.

The Monte Carlo method is flexible enough to remove any or all of the above assumptions, and can be modified to include other effects such as scattering, nongrey and/or nondiffuse walls, etc. These would be extremely difficult to include in other methods.

Monte Carlo is relatively easy to program, and its chief drawback is the large use of computer time in complex cases. However, since this is probably the only way of obtaining solutions in such cases, this use is generally justified.

ACKNOWLEDGMENT

The authors wish to thank Mr. Harold Renkel and Miss Patricia Knoop, who carried out the many complex and tedious computations for this paper.

APPENDIX A

DERIVATION OF MONTE CARLO RELATIONS

Determination of wavelength of bundle emitted from a surface. - The total energy per unit area emitted from surface A is

$$q_A = \int_{\lambda=0}^{\infty} \epsilon_{\lambda A} e_{\lambda b,A} \, d\lambda \tag{A1}$$

and the frequency distribution of energy in a wavelength band $d\lambda$ is

$$f_A(\lambda) = \frac{\epsilon_{\lambda A} e_{\lambda b,A} \, d\lambda}{\int_0^{\infty} \epsilon_{\lambda A} e_{\lambda b,A} \, d\lambda} \tag{A2}$$

Transforming to a uniform density distribution by means of the cumulative distribution function

$$R = \int_0^{\xi} f_A(\xi) d\xi \tag{A3}$$

gives

$$R = \frac{\int_0^{\lambda} \epsilon_{\lambda A} e_{\lambda b,A} \, d\lambda}{\int_0^{\infty} \epsilon_{\lambda A} e_{\lambda b,A} \, d\lambda} \tag{A4}$$

If R is taken as a random number in the range of 0 to 1, then (A4) can be solved for the wavelength of emission λ.

Determination of wavelength of bundle emitted from a gas. - For emission from a gas, a similar procedure yields

$$R = \left[\frac{\displaystyle\int_0^{\lambda} \kappa_\lambda e_{g,\lambda}\, d\lambda}{\displaystyle\int_0^{\infty} \kappa_\lambda e_{g,\lambda}\, d\lambda}\right]_i \tag{A5}$$

Determination of bundle path length to absorption. - The number of bundles dN that will be absorbed in a nondimensional distance dl divided by the number of bundles originally emitted is

$$\frac{dN}{N_0} = \frac{-\tau_\lambda N\, dl}{N_0} = f_n \tag{A6}$$

Solving for N/N_0 and substituting above gives

$$f_n\, dl' = -\tau_\lambda \exp\left[-\int_0^{l'} \tau_\lambda\, dl''\right] dl' = \frac{d}{dl'}\left[\exp\left(-\int_0^{l'} \tau_\lambda\, dl''\right)\right] \tag{A7}$$

This can be transformed to the uniform distribution

$$R = \int_0^{l} f_n\, dl' = 1 - \exp\left[-\int_0^{l} \tau_\lambda\, dl'\right] \tag{A8}$$

Since R is evenly distributed between 0 and 1, it can be replaced by $1 - R$ to give

$$\ln R = -\int_0^{l} \tau_\lambda\, dl' \tag{A9}$$

Point of emission of bundle in gas for gas heat source case. - If an energy distribution of the form given by equation (12) is assumed, the cumulative distribution is

$$R = \frac{\int_0^x G(x')dx'}{\int_0^1 G(x')dx'} = 2x^2[(3/2) - x] \qquad \text{(A10)}$$

It can be shown by Rolle's Theorem and its corollaries [7] that this equation, which must be solved for x in terms of R, has one and only one real root in the range of interest and that this root is

$$x = F_S(R) = \frac{1}{2} + \cos\left(\frac{\Gamma + 4\pi}{3}\right) \qquad \text{(A11)}$$

where

$$\Gamma = \cos^{-1}(1 - 2R) \qquad \text{(A12)}$$

APPENDIX B

MODIFIED DIFFUSION SOLUTION

From the diffusion solution as derived by Deissler [3], the emissive power of a gas near point x can be expressed in a Taylor series as

$$e_{g\lambda}(\zeta) = \sum_{n=0}^{\infty}\left[\frac{1}{n!}(\zeta - x)^n\left(\frac{d^n e_{g\lambda}}{d\zeta^n}\right)_x\right] \tag{B1}$$

for the geometry considered herein.

The emission at wavelength λ from a gas element dV which passes through an elemental area dA from above is

$$dE^+_{\lambda x} = \frac{\kappa_{\lambda,x} e_{g\lambda\zeta}\, dV\, dA \cos\eta \exp[-\kappa_{\lambda,x}\rho]}{\pi\rho^2} \tag{B2}$$

where ρ is the distance between the volume element dV and the plane element dA, and $\kappa_{\lambda,x}$ is assumed constant in the region near point x.

Integrating over the entire volume above dA gives

$$E^+_{\lambda x} \approx \frac{\kappa_{\lambda,x}\, dA}{\pi}\sum_{n=0}^{\infty}\frac{1}{n!}\left(\frac{d^n e_{g\lambda}}{d\zeta^n}\right)_x\int_{\rho=0}^{\infty}\int_{\eta=0}^{\pi/2}\int_{\theta=0}^{2\pi}\rho^n \sin\eta\cos^{n+1}\eta\exp[-\kappa_{\lambda,x}\rho]\,d\theta\, d\eta\, d\rho$$

$$= dA\sum_{n=0}^{\infty}\frac{2}{\kappa^n_{\lambda,x}(n+2)}\left(\frac{d^n e_{g,\lambda}}{d\zeta^n}\right) = dA\sum_{n=0}^{\infty}(\Lambda_{\lambda,x})_n \tag{B3}$$

Similarly, the energy passing through dA from below is

$$E^{-}_{\lambda,x} = dA \sum_{n=0}^{\infty} (-1)^n (\Lambda_{\lambda,x})_n \tag{B4}$$

Then the net radiation per unit area in the direction x at wavelength λ is

$$q_{\lambda,x} = \frac{E^{-}_{\lambda,x} - E^{+}_{\lambda,x}}{dA} = \sum_{n=0}^{\infty} [(-1)^n - 1](\Lambda_{\lambda,x})_n \tag{B5}$$

The terms in the summation in (B5) are 0 for any even n.

To evaluate the jump in emissive power between the gas and the wall at the wall, assume an element dA slightly below wall 1. Then the energy passing downward through dA at wavelength λ

$$\frac{E^{+}_{\lambda 1}}{dA} = e_{\lambda,1} + (1 - \epsilon_{\lambda 1}) \frac{E^{-}_{\lambda 1}}{dA} \tag{B6}$$

Combining (B4), (B5), and (B6), all evaluated at wall 1, gives

$$\frac{q_{\lambda 1}}{\epsilon_{\lambda 1}} = e_{g\lambda,1} - e_{b\lambda,1} + \sum_{n=1}^{\infty} (-1)^n (\Lambda_{\lambda,1})_n \tag{B7}$$

Similarly, for surface 0,

$$\frac{-q_{\lambda 0}}{\epsilon_{\lambda 0}} = e_{g\lambda,0} - e_{b\lambda,0} + \sum_{n=1}^{\infty} (\Lambda_{\lambda,0})_n \tag{B8}$$

If $e_{g,\lambda}$ is neglected to higher order derivatives than 2, (B5) becomes

$$\frac{-4}{3\kappa_{\lambda,x}} \left(\frac{de_{g,\lambda}}{d\zeta}\right)_x = q_{\lambda,x} \tag{B9}$$

Evaluating the boundary conditions under a similar restriction gives

$$\frac{q_{\lambda 1}}{\epsilon_{\lambda 1}} = e_{g\lambda,1} - e_{b\lambda,1} - \frac{2}{3\kappa_{\lambda,1}}\left(\frac{de_{g,\lambda}}{d\zeta}\right)_1 + \frac{1}{2\kappa^2_{\lambda,1}}\left(\frac{d^2e_{g,\lambda}}{d\zeta^2}\right)_1 \tag{B10}$$

$$\frac{-q_{\lambda 0}}{\epsilon_{\lambda 0}} = e_{g\lambda,0} - e_{b\lambda,0} + \frac{2}{3\kappa_{\lambda,0}}\left(\frac{de_{g,\lambda}}{d\zeta}\right)_0 + \frac{1}{2\kappa^2_{\lambda,0}}\left(\frac{d^2e_{g,\lambda}}{d\zeta^2}\right)_0 \tag{B11}$$

Integrating equation (B9) over a wavelength range $\Delta\lambda$ gives

$$\bar{q}_x = \frac{-4}{3\bar{\kappa}_{R,x}}\int_{\Delta\lambda}\left(\frac{de_{g,\lambda}}{d\zeta}\right)_x d\lambda = \frac{-4}{3\bar{\kappa}_{R,x}}\left(\frac{d\bar{e}_g}{d\zeta}\right)_x \tag{B12}$$

where the bar denotes an integration over the wavelength range $\Delta\lambda$.

The Rosseland mean absorption coefficient, $\bar{\kappa}_{R,x}$ is defined by

$$\frac{1}{\bar{\kappa}_{R,x}} \equiv \frac{\displaystyle\int_{\Delta\lambda}\frac{1}{\kappa_{\lambda,x}}\left(\frac{\partial e_{g,\lambda}}{\partial e_g}\right)_x d\lambda}{\displaystyle\int_{\Delta\lambda}\left(\frac{\partial e_{g,\lambda}}{\partial e_g}\right) d\lambda} \tag{B13}$$

Similarly, after substituting (B9) into (B10) and (B11), and assuming grey walls, the boundary conditions are integrated to

$$\bar{e}_{b,1} - \bar{e}_{b,1} = \bar{q}_1\left(\frac{1}{\epsilon_1} - \frac{1}{2}\right) - \frac{1}{2\bar{\kappa}^2_{s,1}}\left(\frac{d^2\bar{e}_g}{d\zeta^2}\right)_1 - \frac{1}{2\bar{I}_1}\left(\frac{d\bar{e}_g}{d\zeta}\right)^2_1 \tag{B14}$$

$$\bar{e}_{b0} - \bar{e}_{g,0} = \bar{q}_0 \left(\frac{1}{\epsilon_0} - \frac{1}{2} \right) + \frac{1}{2\bar{\kappa}^2_{s,0}} \left(\frac{d^2\bar{e}_g}{d\zeta^2} \right)_0 + \frac{1}{2\bar{I}_0} \left(\frac{d\bar{e}_g}{d\zeta} \right)^2_0 \tag{B15}$$

where

$$\frac{1}{\bar{\kappa}^2_{s,x}} = \frac{\displaystyle\int_{\Delta\lambda} \frac{1}{\kappa^2_{\lambda,x}} \left(\frac{\partial e_{g,\lambda}}{\partial e_g} \right)_x d\lambda}{\displaystyle\int_{\Delta\lambda} \left(\frac{\partial e_{g,\lambda}}{\partial e_g} \right) d\lambda} \tag{B16}$$

and

$$\frac{1}{\bar{I}_x} = \frac{\displaystyle\int_{\Delta\lambda} \frac{1}{\kappa^2_{\lambda,x}} \left(\frac{\partial^2 e_{g,\lambda}}{\partial e^2_g} \right)_x d\lambda}{\left[\displaystyle\int_{\Delta\lambda} \left(\frac{\partial e_{g,\lambda}}{\partial e_g} \right)_x d\lambda \right]^2} \tag{B17}$$

The derivative terms in (B13), (B16), and (B17) are found by substitution of e_g for σT_g^4 in Planck's energy distribution, and then taking the appropriate derivative.

If a parabolic heat source distribution of the form of equation (12) is assumed, a heat balance on a gas element of width dx yields for the wavelength band $\Delta\lambda$

$$\bar{q}_x = 4DG_{max} \left(\frac{x^2}{2} - \frac{x^3}{3} \right) + \bar{q}_0 \tag{B18}$$

The optical thickness of the gas may be assumed of the form

$$\bar{\tau}_{R,x} = Ax^2 + Bx + C \tag{B19}$$

Higher-order terms could be used if necessary for a specific problem. An iterative solution is necessary, since a temperature distribution must be known to evaluate the constants in (B19).

Using (B19) and (B18) to integrate (B12) and evaluating the boundary conditions, we find after lengthy algebraic manipulation that the heat transferred for the no heat source case with walls at different temperatures is

$$\left(\frac{(q_{0-1})_{net}}{e_{b0} - e_{b1}}\right)_{G(x)=0} = \left(8 + 2A + 3B + 6C + \frac{6A}{\bar{\tau}^2_{s,1}} + 3B\left(\frac{1}{\bar{\tau}^2_{s,1}} - \frac{1}{\bar{\tau}^2_{s,0}}\right)\right.$$

$$- \left\{\left[8 + 2A + 3B + 6C + \frac{6A}{\bar{\tau}^2_{s,1}} + 3B\left(\frac{1}{\bar{\tau}^2_{s,1}} - \frac{1}{\bar{\tau}^2_{s,0}}\right)\right]^2\right.$$

$$\left.\left. + 72\left[\frac{C^2}{\bar{I}_0} - \frac{(A+B+C)^2}{\bar{I}_1}\right](\bar{e}_{b0} - \bar{e}_{b1})\right\}^{1/2}\right) \Bigg/ \frac{-9}{2D^2}(e_{b0} - e_{b1})\left[\frac{C^2}{\bar{I}_0} - \frac{(A+B+C)^2}{\bar{I}_1}\right] \tag{B20}$$

A correction added to the heat transfer needed to include that energy outside the wavelength band considered is

$$\left[\frac{(q_{0-1})_{net}}{e_{b0} - e_{b1}}\right]_{correction} = 1 - \frac{\int_{\lambda_{min}}^{\lambda_{max}} (e_{b\lambda 0} - e_{b\lambda 1})d\lambda}{(e_{b0} - e_{b1})} \tag{B20a}$$

This correction had a value of 0.0212 for the wall temperatures in the example.

The emissive power distribution for the same case is

$$\left(\frac{\bar{e}_{g,x} - e_{b0}}{e_{b1} - e_{b0}}\right)_{G(x)=0} = \left(\frac{\bar{q}_0}{e_{b0} - e_{b1}}\right)\left[\frac{Ax^3}{4} + \frac{3Bx^2}{8} + \frac{3Cx}{4} + \frac{1}{2} - \frac{3B}{8\bar{\tau}_{s,0}^2}\right]$$

$$+ \frac{\bar{e}_{b0} - e_{b0}}{e_{b1} - e_{b0}} + \frac{9C^2(e_{b0} - e_{b1})}{32\bar{I}_0 D^2}\left(\frac{\bar{q}_0}{e_{b0} - e_{b1}}\right)^2 \qquad \text{(B21)}$$

For a parabolic heat source between black walls at equal temperatures,

$$\left(\frac{e_{g,x} - e_b}{\frac{2DG_{max}}{3}}\right)_{T_0=T_1} = \frac{1}{4} - \frac{3C^2G_{max}}{64\bar{I}_0 D} - \frac{3B}{16\bar{\tau}_{s,0}^2} + \frac{x}{8}\left(Ax^2 + \frac{3Bx}{2} + 3C\right)$$

$$+ \frac{\bar{e}_b - e_b}{\frac{2DG_{max}}{3}} + \frac{3x^3}{4}\left[\frac{Ax^3}{3} - \frac{x^2(3A - 2B)}{5} - \frac{x(3B - 2C)}{4} - C\right]$$

(B22)

In order to find the total heat transferred between the two surfaces for the example problem, the correction given by equation (B20a) must be added to (B20). To find the total emissive power at point x in the gas, $e_{g,x}$, a correction must be applied to equations (B21) and (B22) to change $\bar{e}_{g,x}$ to $e_{g,x}$. This correction is given by

$$\frac{\bar{e}_{g,x}}{e_{g,x}} = \frac{\int_{\Delta\lambda} e_{g\lambda,x}\, d\lambda}{\sigma T_x^4} \qquad \text{(B22a)}$$

The constants A, B, and C in equations (B19) to (B22) were calculated at $x = 0$, 0.5, and 1 for the solution given.

For the no gas heat source case, the limiting solution for large D can be found from equation (B12) since there is no jump in the wall boundary conditions. The solution is

$$\left(\frac{\bar{e}_{g,x} - \bar{e}_{b0}}{\bar{e}_{b1} - \bar{e}_{b0}}\right)_{D\to\infty} = \frac{\int_0^x \bar{\kappa}_R(x)\ dx}{\int_0^1 \bar{\kappa}_R(x)\ dx} \tag{B23}$$

This solution is also iterative, and is exact in the limit $D \to \infty$. Again the emissive power e must be obtained from the ratio $\bar{e}/e$ given by equation (B22a).

APPENDIX C

TRANSPARENT GAS APPROXIMATION

If we assume the plate spacing D small enough that the gas optical thickness in any element $\tau_{\lambda,i}$ is small, we can neglect the attenuation of energy in the gas. An energy balance on an isothermal element Δx then gives

$$4\tau_{\lambda,x}e_{g\lambda,x}\,d\lambda = 2\tau_{\lambda,x}(e_{b0,\lambda} + e_{b1,\lambda})d\lambda + D[G(x)]_{\lambda}\,d\lambda \tag{C1}$$

for the general problem of black surfaces at unequal temperatures enclosing a real gas with distributed energy sources. For no energy sources, integrating over all wavelengths yields

$$e_{g,x} = \frac{1}{2\tau_{P,x}}\int_0^{\infty} \tau_{\lambda,x}\,(e_{b0,\lambda} + e_{b1,\lambda})d\lambda \tag{C2}$$

For equal surface temperatures and a parabolic heat source distribution,

$$e_{g,x} = \frac{1}{\tau_{P,x}}\left[\int_0^{\infty} \tau_{\lambda,x}e_{b\lambda}\,d\lambda + DG_{max}x(1 - x)\right]$$

E-2013

REFERENCES

1. Hottel, H. C., and Cohen, E. S.: Radiant Heat Exchange in a Gas-filled Enclosure: Allowance for Nonuniformity of Gas Temperature. AIChE Jour. 4, no. 1, 3-14, Mar. (1958).

2. Bevans, J. T., and Dunkle, R. V.: Radiant Interchange Within an Enclosure. ASME Trans., Jour. Heat Transfer, 82, no. 1, 1-19, Feb. (1960).

3. Deissler, R. G.: Diffusion Approximation for Thermal Radiation in Gases with Jump Boundary Condition. Submitted to ASME Trans., Jour. Heat Transfer.

4. Howell, J. R., and Perlmutter, M.: Monte Carlo Solution of Thermal Transfer Through Radiant Media Between Gray Walls. Paper 62-H-116, ASME, 1962. (To be pub. in ASME Trans., Jour. Heat Transfer.)

5. Perlmutter, M., and Howell, J. R.: Radiant Transfer Through a Gray Gas Between Concentric Cylinders Using Monte Carlo. Submitted to ASME Trans., Jour. Heat Transfer.

6. Wahl, B. W., Gould, R. J., and McKee, J. W.: Radiative Properties of Hydrogen and Radiative Transfer to the Environment at Elevated Temperatures. Proc. of 4th Biennial Gas Dynamics Symposium. Pub. Northwestern Univ. and ARS, Aug. (1961).

7. Conkwright, N. B.: "Introduction to the Theory of Equations." Ginn and Co., Columbus (1941).

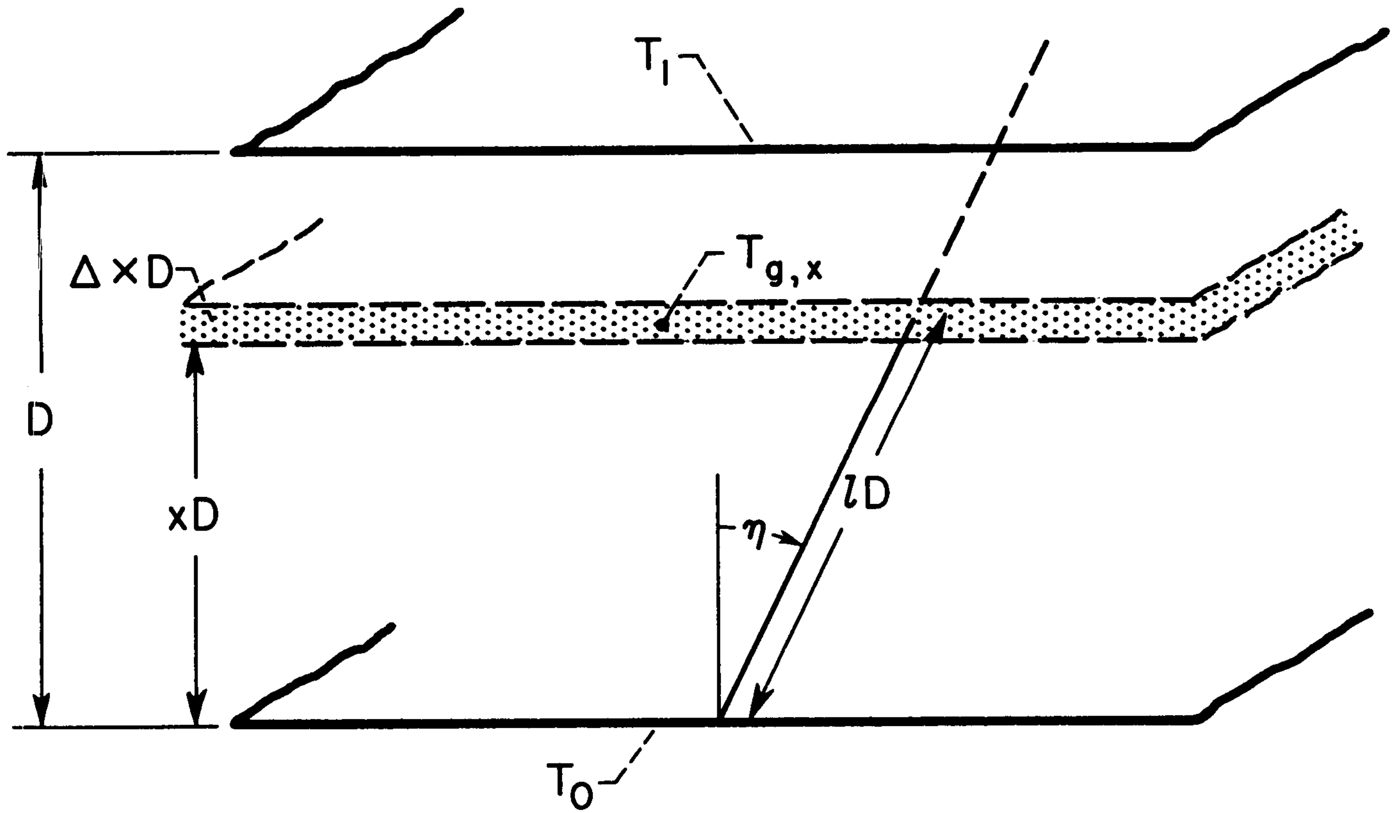

Figure 1. - Geometry for nongrey nonisothermal gas between infinite parallel black plates.

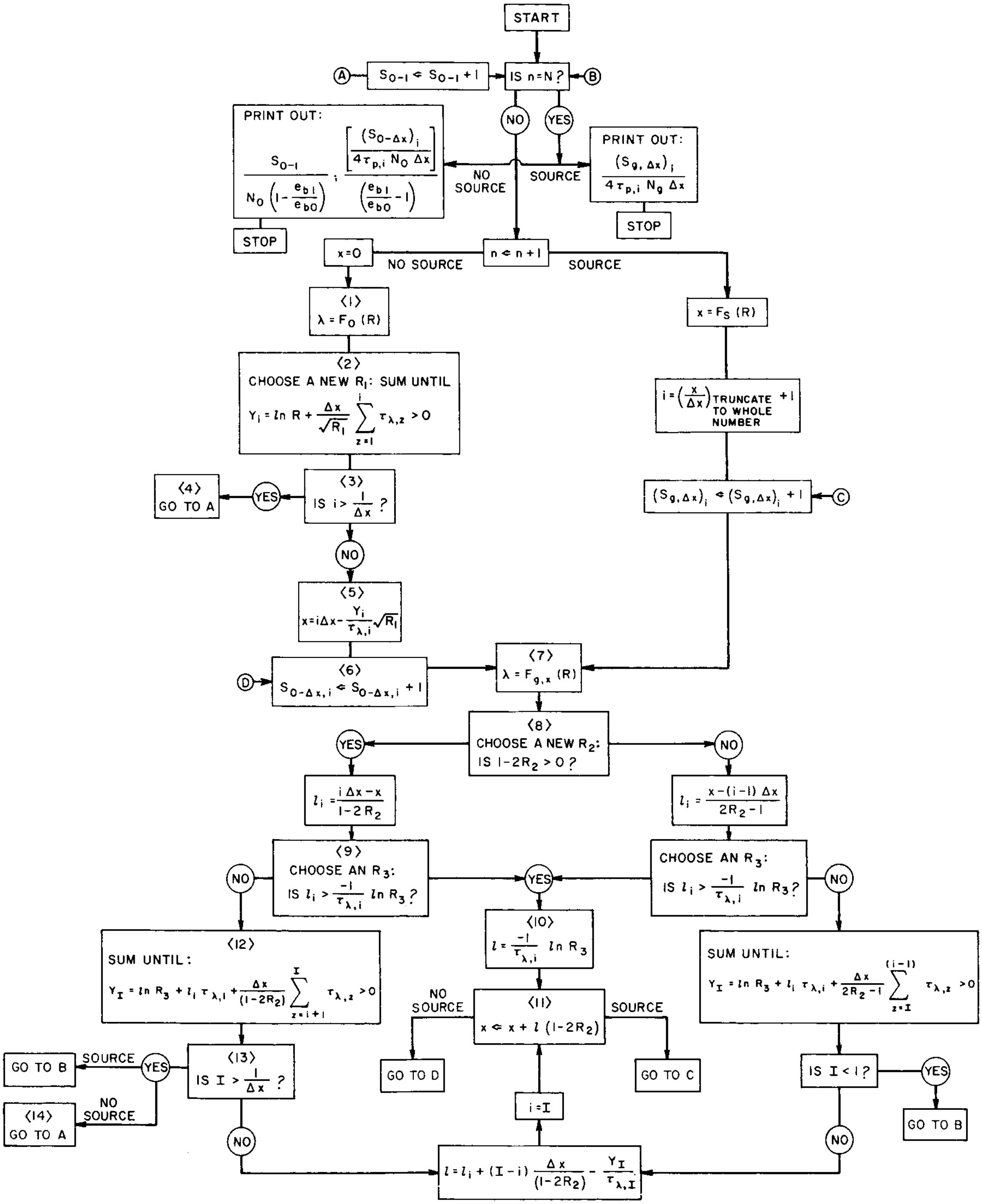

Figure 2. - Computer flow chart.

E-2013

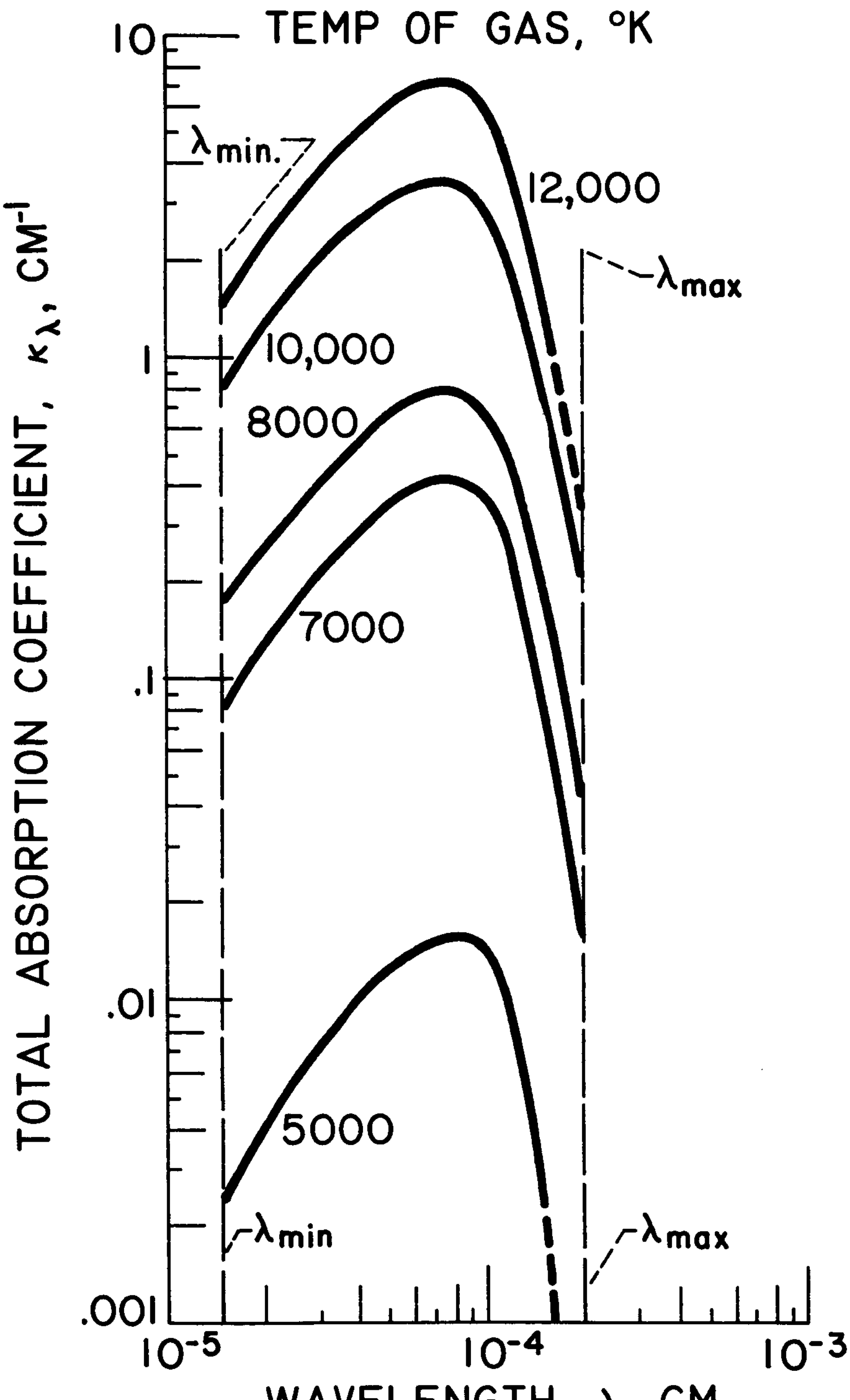

(a) Total absorption coefficient of hydrogen gas at P = 1000 atm (from ref. (6)).

Figure 3. - Properties of hydrogen gas.

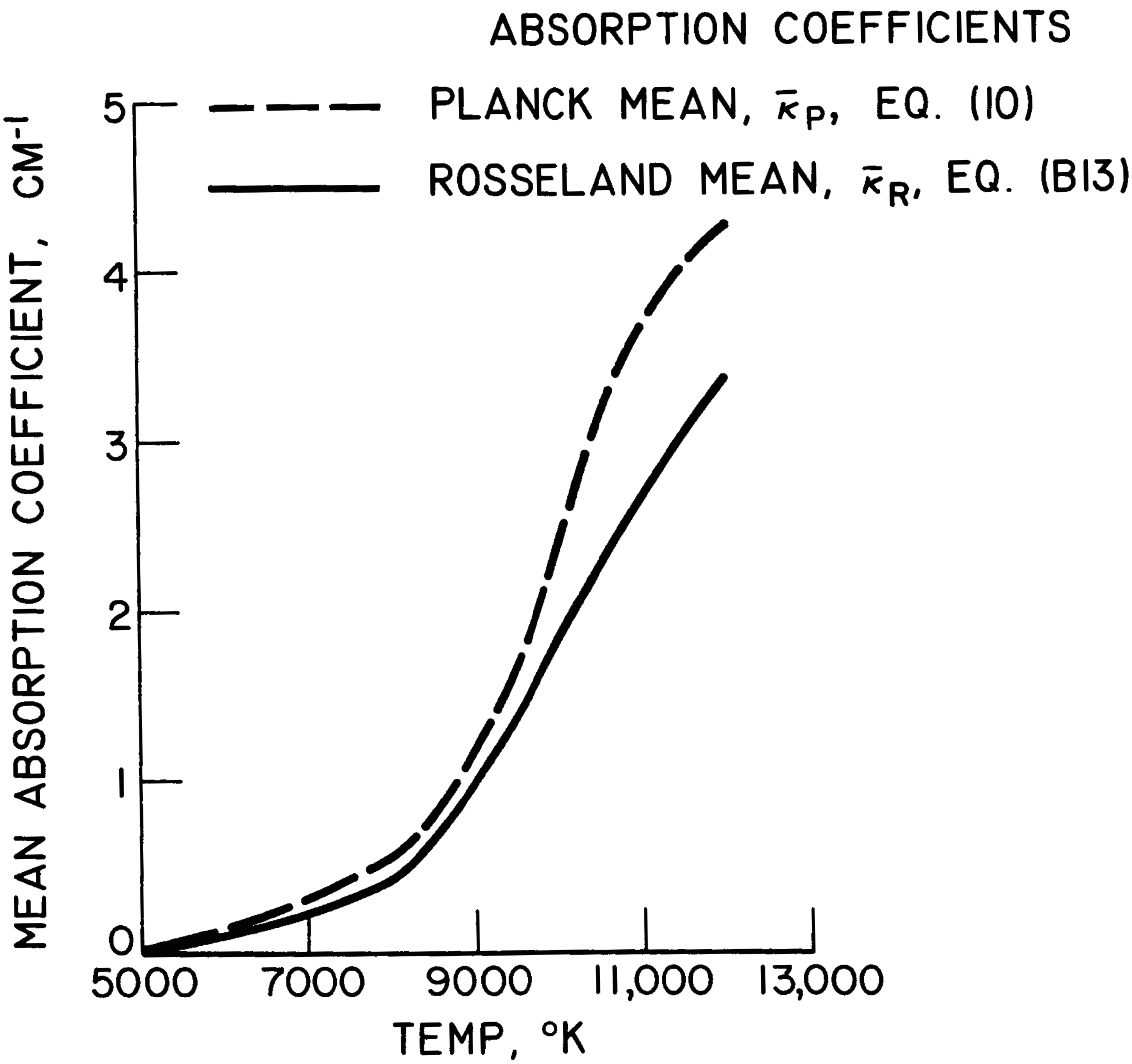

(b) Comparison of mean absorption coefficients for data of figure 3(a); wavelength range, $1.5 \times 10^{-5} < \lambda < 2.0 \times 10^{-4}$ cm.

Figure 3. - Concluded. Properties of hydrogen gas.

E-2013

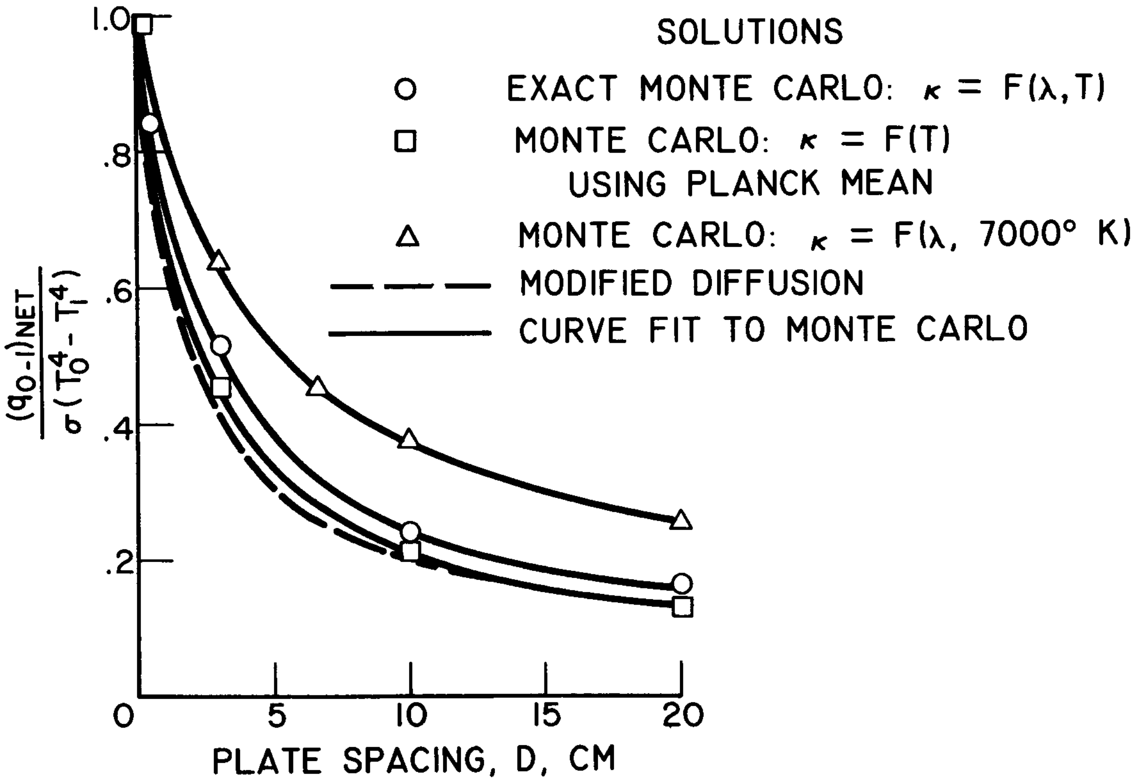

Figure 4. - Heat transfer through hydrogen between black plates; no gas heat source. Plate temperatures: T_0 = 9500° K; T_1 = 4500° K.

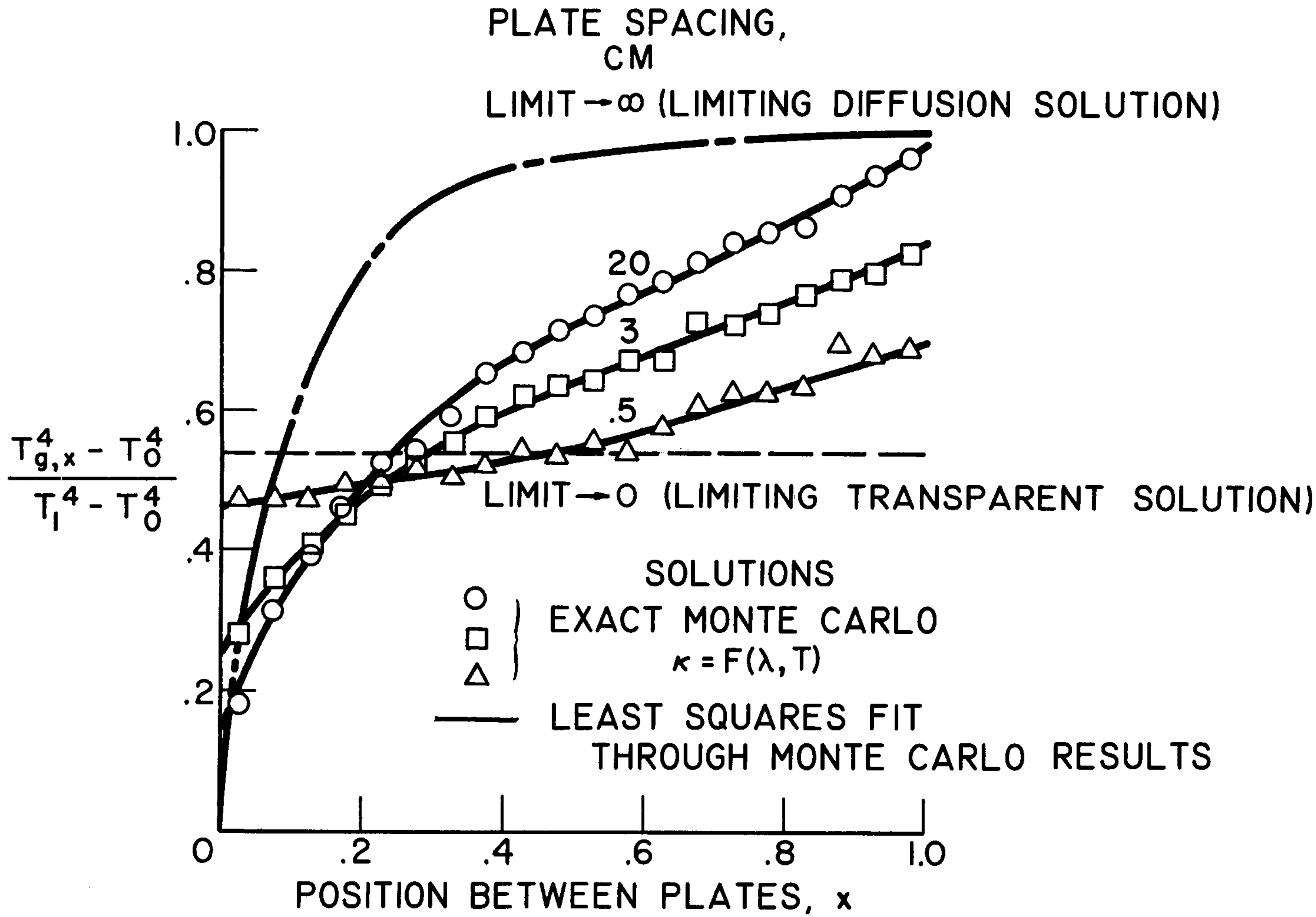

(a) Exact solutions; various spacings.

Figure 5. - Emissive power distribution in hydrogen between parallel plates; no gas heat source; plate temperatures: T_0 = 9500° K; T_1 = 4500° K.

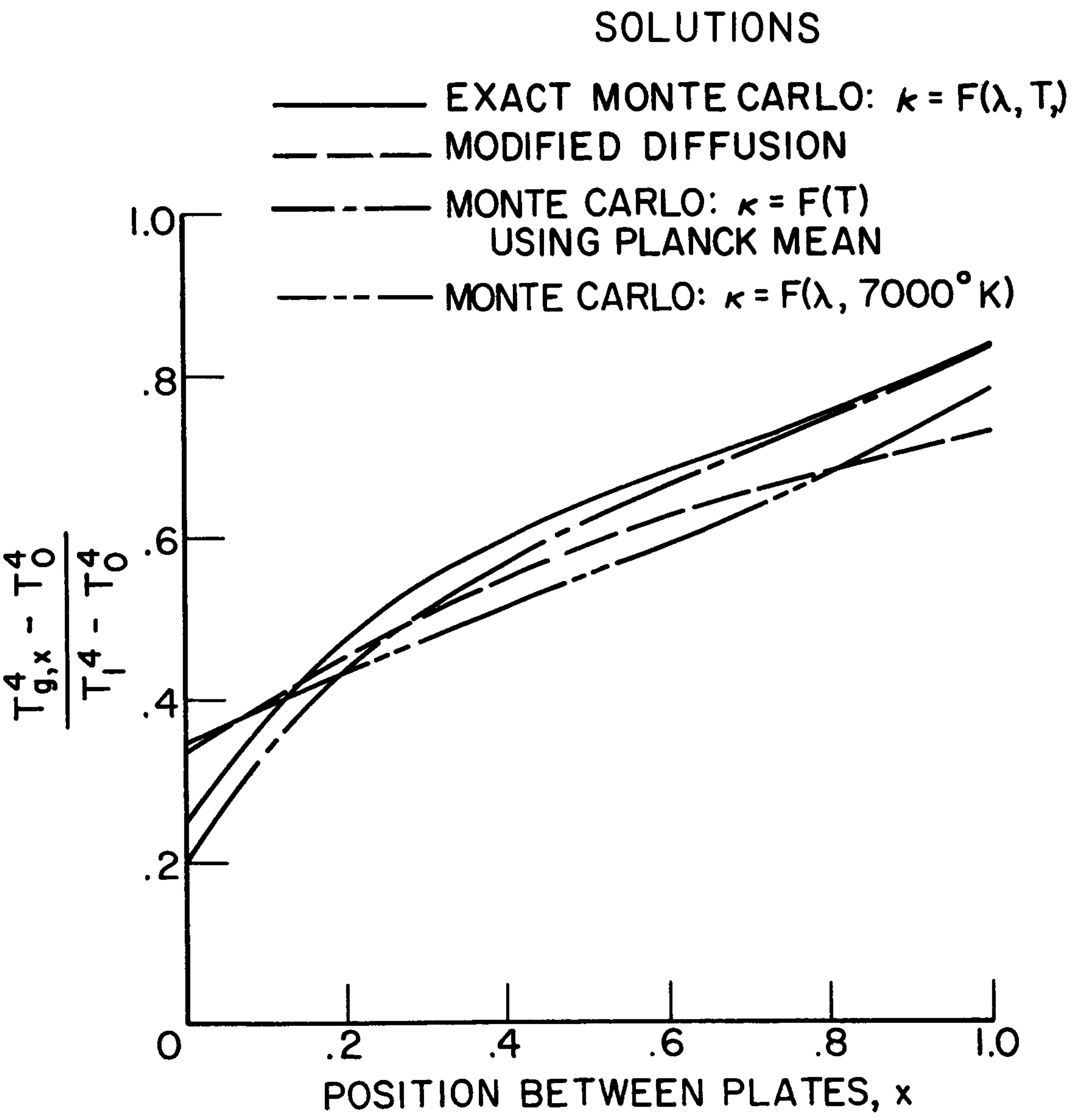

(b) Plate spacing, 3 cm.

Figure 5. - Continued. Emissive power distribution in hydrogen between parallel plates; no gas heat source; plate temperatures: T_0 = 9500° K; T_1 = 4500° K.

E-2013

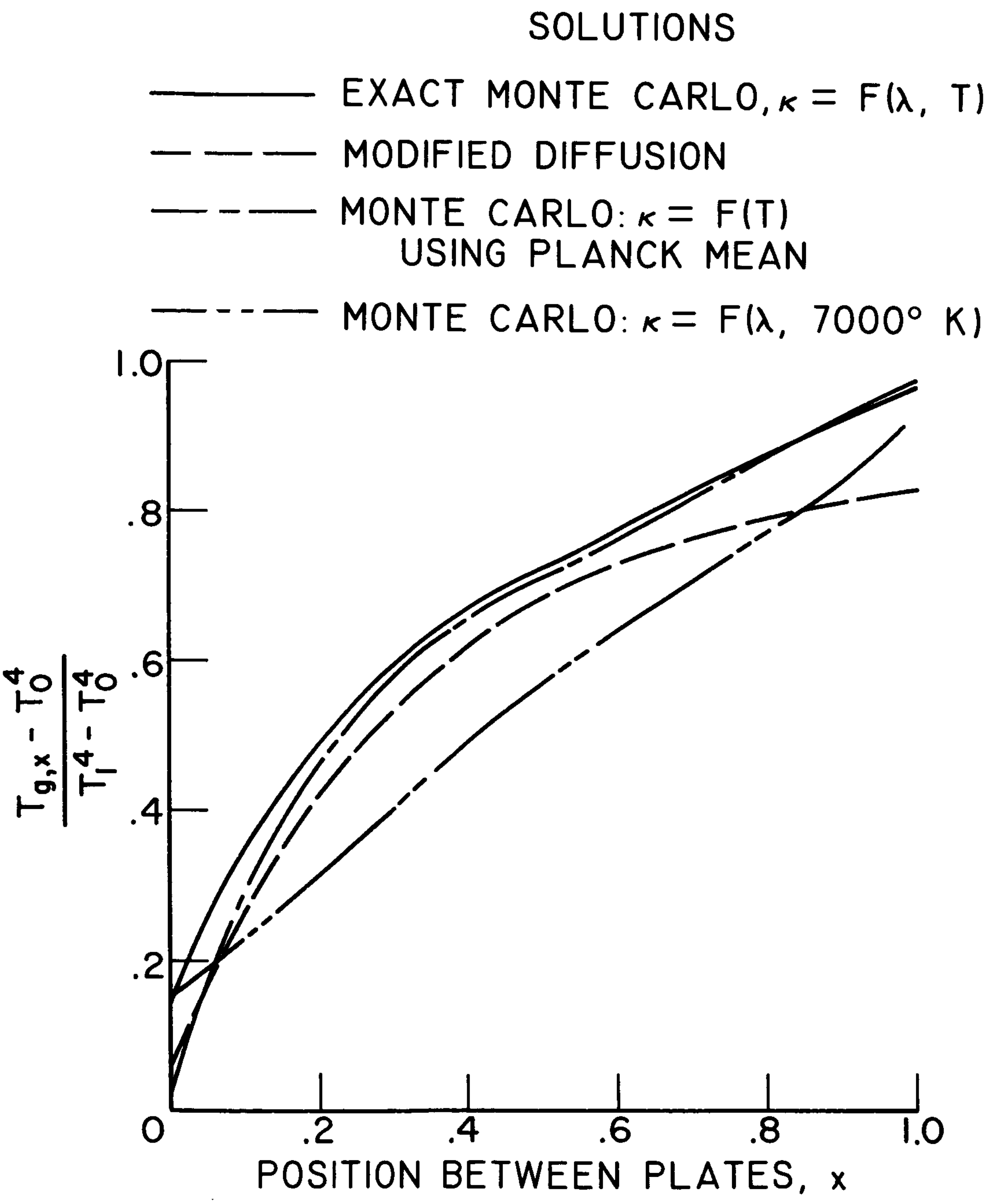

(c) Plate spacing, 20 cm.

Figure 5. - Concluded. Emissive power distribution in hydrogen between parallel plates; no gas heat source; plate temperatures: $T_0 = 9500^\circ$ K; $T_1 = 4500^\circ$ K.

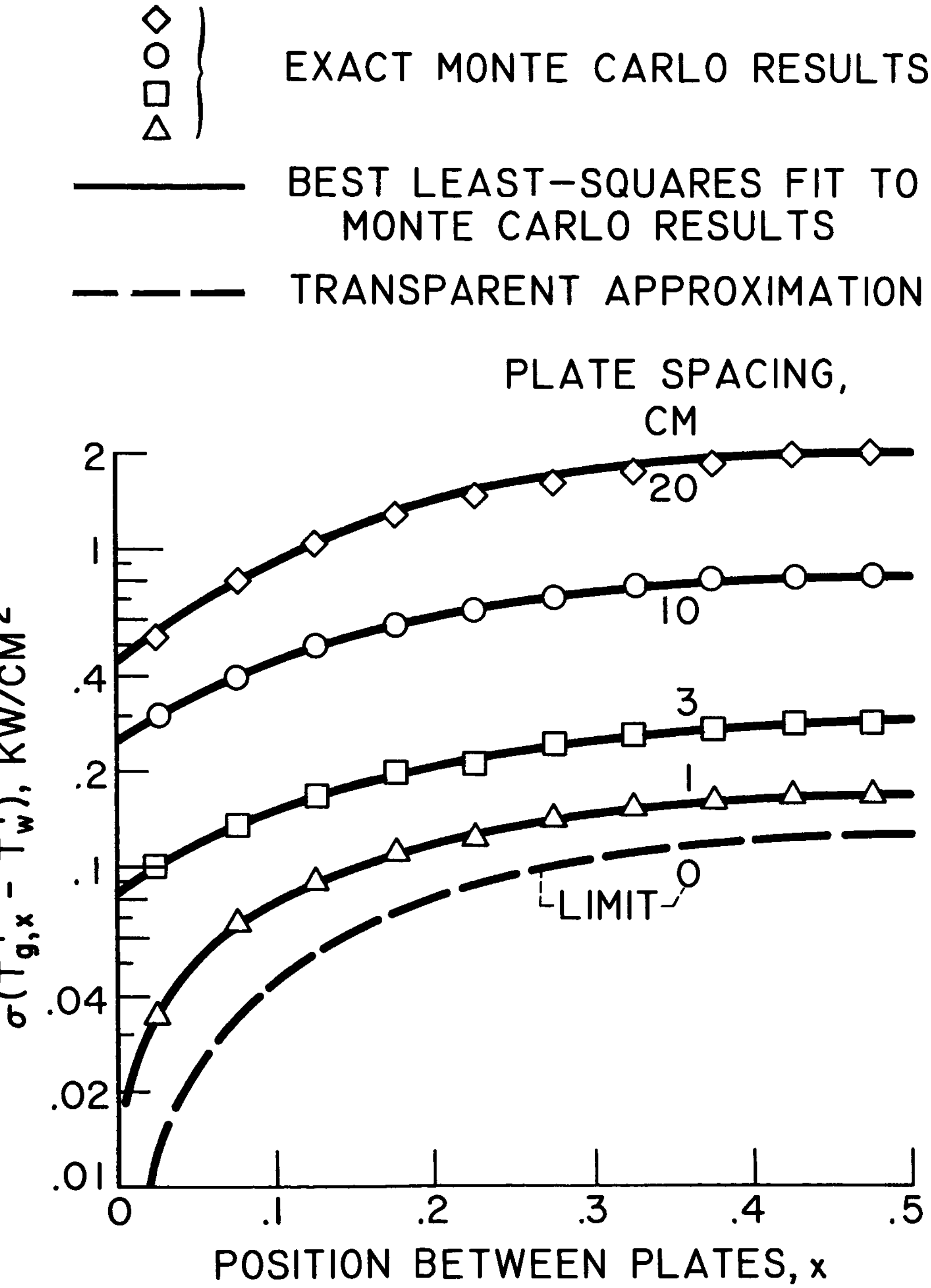

(a) Exact solution; various plate spacings.

Figure 6. - Emissive power distribution in hydrogen between parallel black plates; parabolic heat source; plate temperatures: $T_W = T_0 = T_1 = 7000^\circ$ K; $G_{MAX} = 0.145$ kw/cm^3.

E-2013

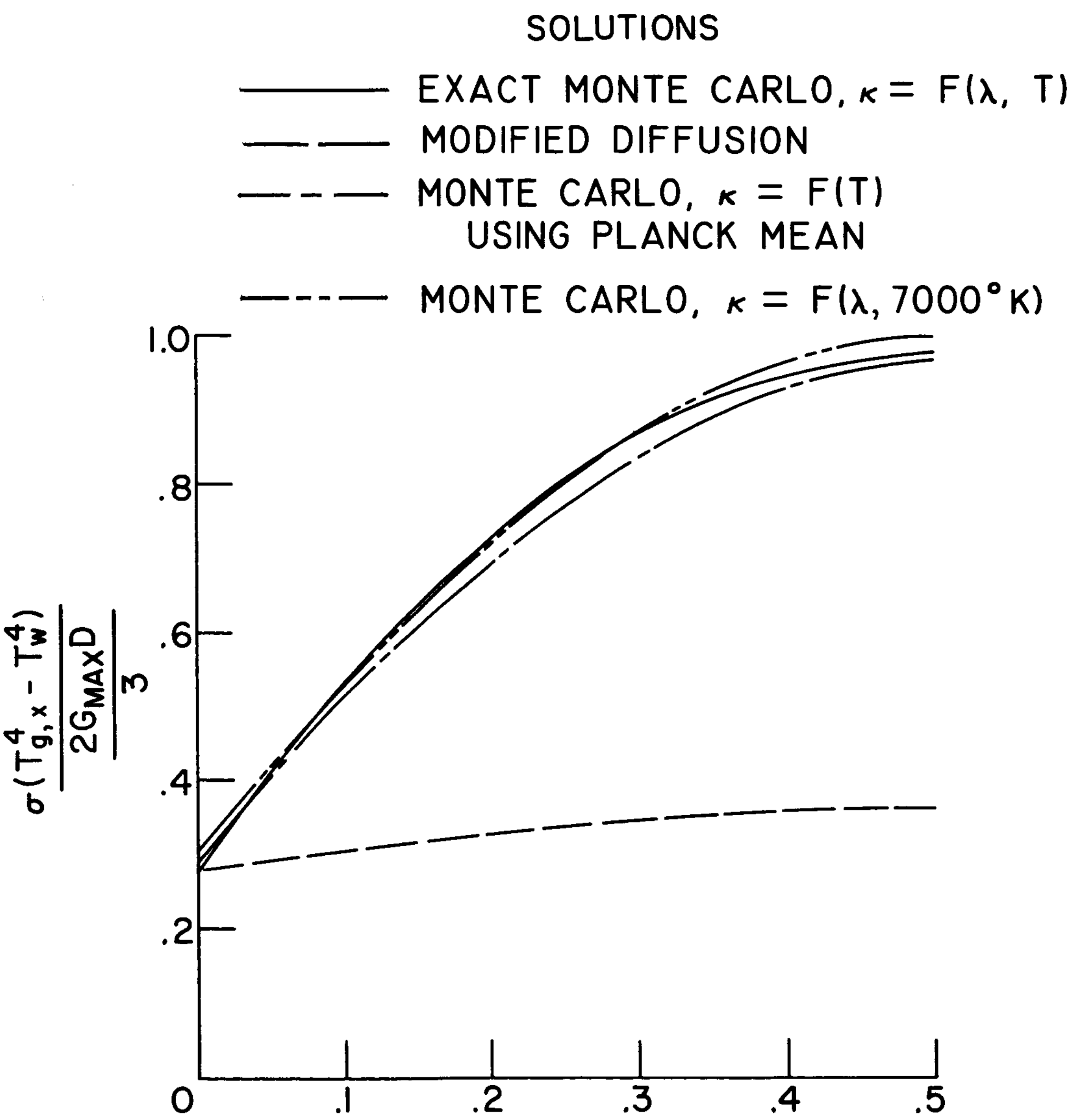

(b) Plate spacing, 3 cm.

Figure 6. - Continued. Emissive power distribution in hydrogen between parallel black plates; parabolic heat source; plate temperatures: $T_w = T_0 = T_1 = 7000^\circ$ K; $G_{MAX} = 0.145$ kw/cm^3.

E-2013

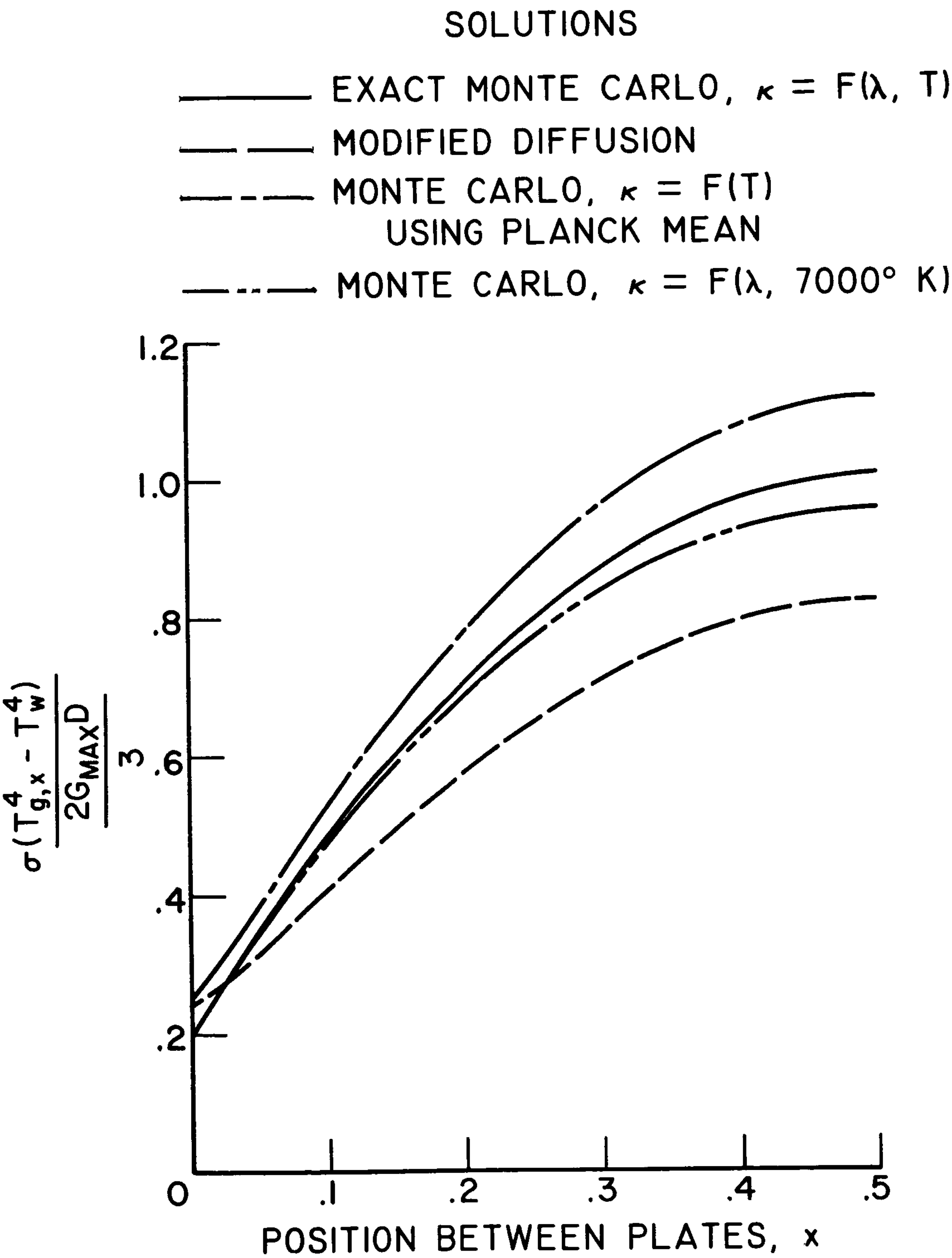

(c) Plate spacing, 20 cm.

Figure 6. - Concluded. Emissive power distribution in hydrogen between parallel black plates; parabolic heat source; plate temperatures: $T_W = T_0 = T_1 = 7000^\circ$ K; $G_{MAX} = 0.145$ kw/cm^3.

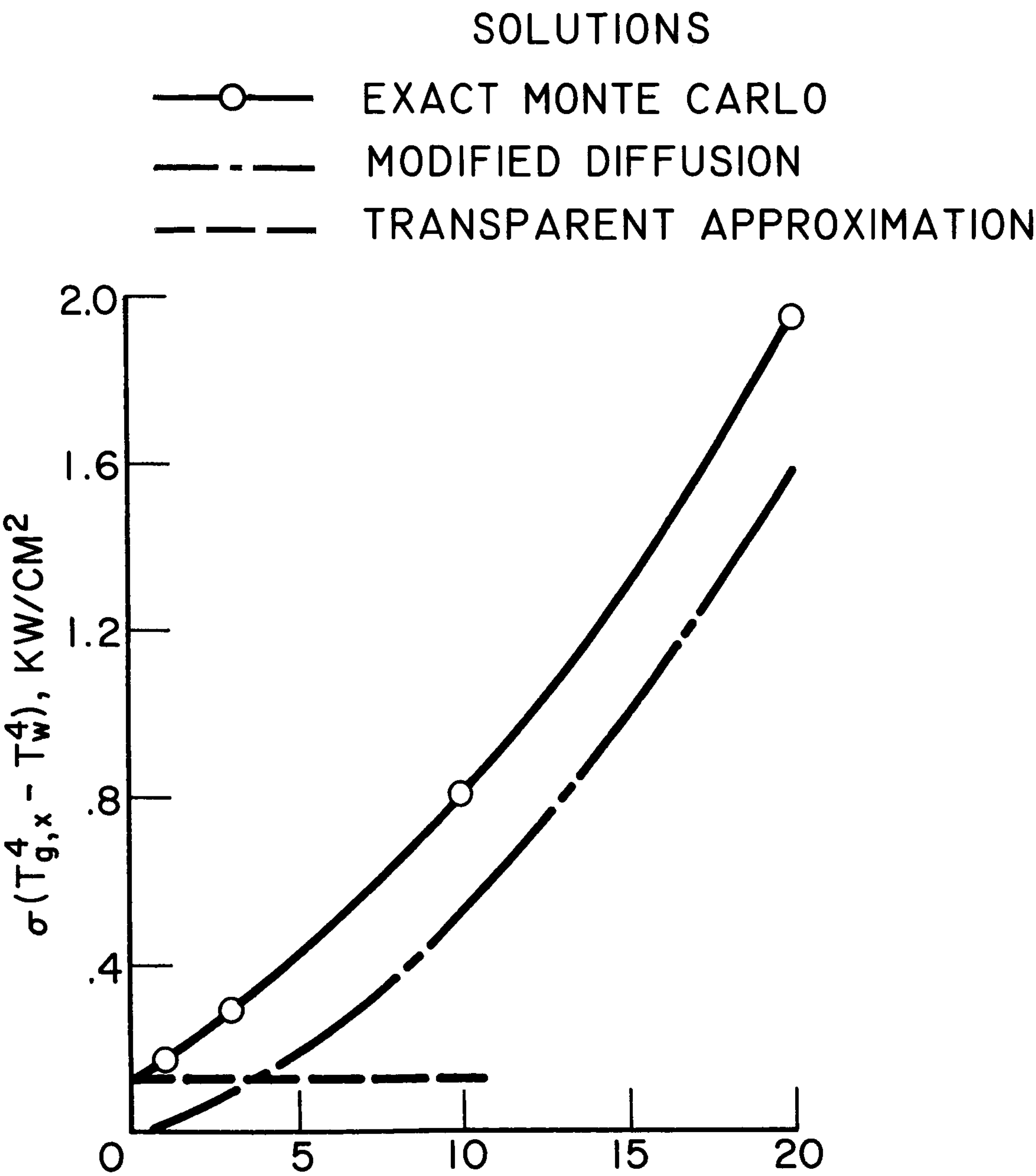

Figure 7. - Comparison of approximations for large and small plate spacing; parabolic source case; plate temperatures: $T_W = T_0 = T_1 = 7000^{\circ}$ K; $G_{MAX} = 0.145$ kw/cm^3.